Deep-Sea Research I 58 (2011) 915–921

Contents lists available at ScienceDirect

Deep-Sea Research I

journal homepage: www.elsevier.com/locate/dsri

Projecting uncertainty onto marine megafauna trajectories

Alexander A. Robel [a,*], M. Susan Lozier [a], Stefan F. Gary [a], George L. Shillinger [b], Helen Bailey [c,1], Steven J. Bograd [c]

[a] Division of Earth and Ocean Sciences, Nicholas School of the Environment, Duke University, P.O. Box 90227, Durham, NC 27708, USA
[b] Center for Ocean Solutions, Stanford University, 99 Pacific Street, Suite 155A, Monterey, CA 93940, USA
[c] Environmental Research Division, NOAA Southwest Fisheries Science Center, 1352 Lighthouse Avenue, Pacific Grove, CA 93950, USA

ARTICLE INFO

Article history:
Received 10 February 2011
Received in revised form
23 June 2011
Accepted 27 June 2011
Available online 3 July 2011

Keywords:
Marine megafauna pathways
Active & passive migration
Pathway uncertainty
Biologging
Sea turtles

ABSTRACT

In this study, a method is proposed for estimating the uncertainty of a Lagrangian pathway calculated from an undersampled ocean surface velocity field. The primary motivation and application for this method is the differentiation between active and passive movements for sea turtles whose trajectories are observed with satellite telemetry. Synthetic trajectories are launched within a reconstructed surface velocity field and integrated forward in time to produce likely trajectories of an actual turtle or drifter. Uncertainties in both the initial conditions at launch and the velocity field along the trajectory are used to yield an envelope of possible synthetic trajectories for each actual trajectory. The juxtaposition of the actual trajectory with the resulting cloud of synthetic trajectories provides a means to distinguish between active and passive movements of the turtle. The uncertainty estimates provided by this model may lead to improvements in our understanding of where and when turtles are engaged in specific behaviors (i.e. migration vs. foraging)—for which potential management efforts may vary accordingly.

1. Introduction

The development of long-term strategies for ocean ecosystem management depends crucially on our understanding of the migratory behavior of marine species. A series of recent studies (Godley et al., 2008) have utilized electronic tracking information to make inferences about foraging and migration habitats for a variety of pelagic species, including sea turtles and other marine megafauna. As marine spatial planning efforts evolve to address protection of these species within distant high sea habitats (Ardron et al., 2008; Game et al., 2009), our ability to accurately record and interpret animal behaviors and movements will become increasingly valuable.

In a study focused on sea turtle movement, Gaspar et al. (2006) (hereafter G06) proposed a method for distinguishing a turtle's "active" movement (due to deliberate organismal behavior) from its "passive" movement (due to advection by the background flow field). At each observed location along the track of a turtle, G06 subtract the local ocean surface velocity from the turtle's velocity, with the former reconstructed from satellite observations of the surface wind and ocean height fields and the latter from the turtle's position fixes. These velocity anomalies are utilized to calculate a "current-corrected" trajectory from which G06 derive a variety of metrics indicating the extent of deliberate sea turtle behavior, such as the straightness index (Benhamou, 2004). These behavior metrics potentially indicate when a particular turtle is foraging or when it is simply migrating. Aggregation of this information for a number of turtles potentially aids the identification of ocean hotspots for foraging.

Application of the G06 method to the daily ARGOS positions of two (of 46) eastern Pacific leatherback turtles tagged at Playa Grande, Costa Rica during 2004–2007 (Bailey et al., 2008; Shillinger et al., 2008, 2010), is illustrated in Fig. 1. A nine-month-long turtle trajectory in the eastern Pacific (red line in Fig. 1a) is approximately coincident with its current-corrected trajectory (green line), an indication of deliberate or active movement of the turtle. Initially, the turtle moves southward and westward against a weak prevailing eastward surface current (depicted by the blue vectors). Though the surface currents switch from predominantly northwestward to weakly eastward along the path of the turtle, the turtle maintains a southerly track until it turns northward near 27°S. Overall, the turtle's movement would be considered active since the character of its trajectory in the absence of a flow field is remarkably similar to its actual trajectory. This characterization stands in contrast to the turtle movement shown in Fig. 1b, where the actual trajectory (red line) is largely

* Corresponding author. Present address: Department of Earth and Planetary Sciences, Harvard University, 20 Oxford St., Cambridge, MA 02138, USA. Tel.: +1 305 519 0643.
E-mail addresses: alexander.robel@duke.edu, aar11@duke.edu (A.A. Robel), mslozier@duke.edu (M.S. Lozier), stefan.gary@duke.edu (S.F. Gary), georges@stanford.edu (G.L. Shillinger), hbailey@umces.edu (H. Bailey), Steven.Bograd@noaa.gov (S.J. Bograd).
[1] Present address: Chesapeake Biological Laboratory, University of Maryland Center for Environmental Science, 1 Williams Street, P.O. Box 38 Solomons, MD 20688, USA.

0967-0637/$ - see front matter © 2011 Elsevier Ltd. All rights reserved.
doi:10.1016/j.dsr.2011.06.009

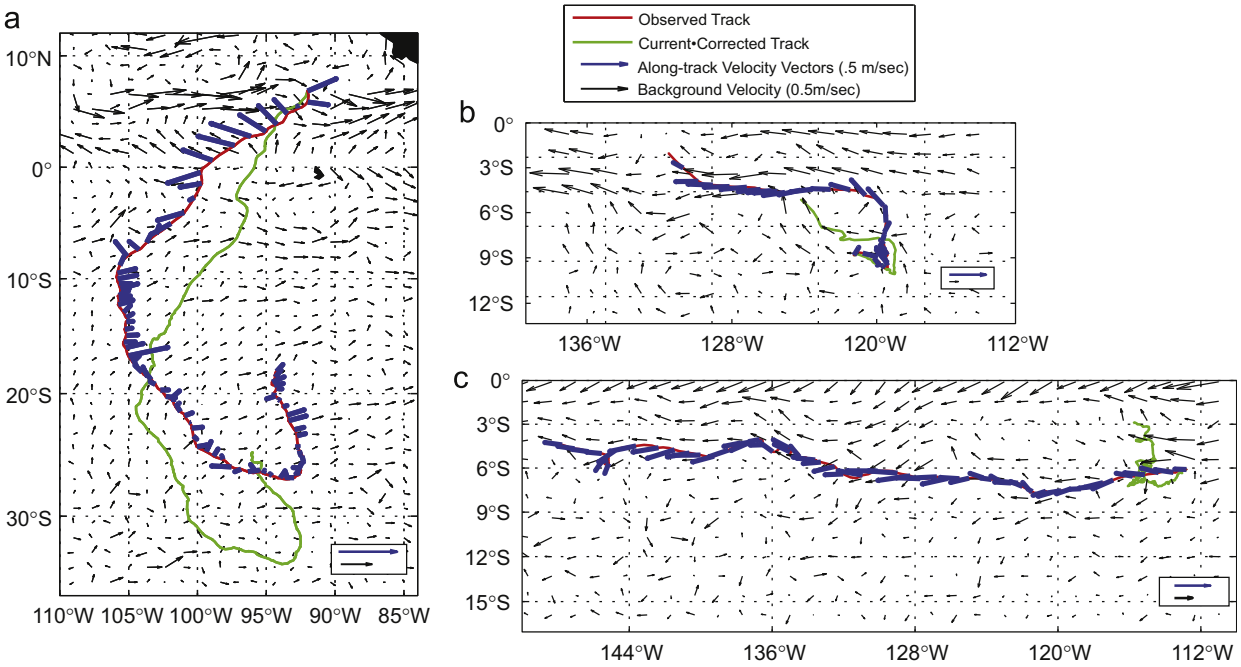

Fig. 1. Trajectories for (a) a sea turtle in the eastern equatorial Pacific (252 days long), (b) a sea turtle in the central equatorial Pacific (63 days long), and (c) a surface drifter (196 days long). Observed trajectories are in red with instantaneous, local satellite-derived surface velocity denoted with blue quivers. Current-corrected trajectories are green. The current-corrected trajectory results from integrating the series of velocities derived from subtracting the surface velocity (blue quiver) from the velocity of the turtle or drifter. Black background vectors depict the average of the reconstructed velocity field over the length of the trajectory.

divergent from the current-corrected trajectory (green line). The turtle trajectory instead is generally aligned with the reconstructed surface currents, indicating turtle movement that is by and large passive.

In the application of the G06 method, the mismatch between the turtle's velocity and the reconstructed surface velocity is assumed to result from active turtle movement. However, another source of mismatch stems from small, unresolved features in the satellite data sets used to reconstruct the surface velocities. Motion at temporal and spatial scales smaller than the spatiotemporal grid of the reconstructed velocity fields, such as sub-mesoscale eddies, may introduce considerable uncertainty in the determination of a current-corrected path. To make this point, the G06 method is applied to the 196-day trajectory of a surface drifter (from the Global Drifter Program) drogued at 40-m in the equatorial Pacific. Ideally, there would be no current-corrected trajectory (green line) since the drifter is, by design, passive. However, the presence of a current-corrected trajectory for this passive drifter (green line in Fig. 1c) demonstrates the impact of undersampling on our interpretation of current-corrected trajectories. A trajectory calculated using an undersampled velocity field could accumulate considerable error over its length, diverging from an actual trajectory in weeks or even days. The divergence could be entirely due to undersampling of the velocity field rather than any deliberate turtle movement. As such, the interpretation of a current-corrected track, such as that depicted in Fig. 1b, is problematic. Accounting for such uncertainty in reconstructed trajectories will considerably aid efforts to realistically separate passive from active movement of marine megafauna. These distinctions could influence the siting of adaptive temporal–spatial management efforts (i.e. time–area closures, gear restrictions) within neritic and pelagic ocean habitats.

This study aims to distinguish active and passive behavior in satellite-tracked turtle trajectories by taking into account the uncertainty that arises from subgrid-scale motions not captured in coarse satellite-derived measures of the ocean surface velocity. We use a reconstruction of the ocean surface velocity composited from estimates of geostrophic and Ekman velocities to produce clouds of simulated passive trajectories that place bounds on the expected movement of a passive turtle. If a turtle's pathway is within these bounds, we cannot make any determination as to whether the turtle is passive or active. However, if the turtle pathway is outside these expected bounds, its movement can be considered deliberate. Since these bounds are dynamic in that they change along the length of the trajectory, this method allows for a determination of when and where an individual turtle transitions between active and passive movements.

2. Methods

The central method developed in this study is for the production of a cloud of simulated passive tracks, termed "synthetic trajectories". In this section, we describe how the surface velocity field is reconstructed from satellite data and then used to create these synthetic trajectories. The method for incorporating uncertainty resulting from unresolved subgrid-scale motions in the velocity field is also described below.

2.1. Reconstruction of surface velocity fields

A local surface velocity in the area of either a passive drifter or turtle trajectory is reconstructed from the sum of geostrophic and Ekman velocities. The geostrophic velocity fields, produced from altimeter-derived sea surface heights, are provided by AVISO (http://www.aviso.oceanobs.com) on a spatial grid of 1/3°, sampled at weekly intervals. The Ekman velocity fields are derived from QuikSCAT wind stress data using the Rio and Hernandez (2003) (hereafter RH03) formulation:

$$\vec{u} = \beta_\tau f^{-1/2} e^{i\theta} \quad (1)$$

where u_e is the Ekman velocity vector, β is an empirical "amplitude factor" estimated in Figure 8 of RH03 to be 0.005 $m^2\,kg^{-1}\,s^{1/2}$ in the eastern tropical Pacific (with a global range of 0.001–

$0.01\ m^2\ kg^{-1}\ s^{1/2}$), $\boldsymbol{\tau}$ is the wind stress vector (in the form $\tau_x + i\tau_y$), f is the Coriolis parameter and θ is an empirical parameter defining the relative direction between the surface velocity and wind stress vectors. The QuikSCAT wind stress field has a spatial resolution of ½°, sampled at daily intervals.

An important part of reconstructing Ekman velocities is selecting an appropriate value for θ. RH03 showed that θ is variable in both space and time, particularly in the equatorial ocean (the location of the three trajectories shown in Fig. 1) where wind stress significantly determines surface velocities in the absence of a strong geostrophic current.[2] In the absence of an empirical relationship for θ that is temporally and spatially variable, we opt to calibrate this parameter to 120° for our study region using the criterion that the calculated surface velocities should optimally align with the passive drifter used here (see Fig. 1c). RH03 find θ in the surface waters of the equatorial Pacific to be in the range 50–90°. Their study notes that discrepancies between studies are expected given the use of data over shorter intervals and the interannual variability of wind forcing. Such a discrepancy might also be explained by the fact that the passive drifter was drogued at 40 m. As such, the clockwise rotation of the Ekman velocity with depth and the calibration over a much shorter time interval than RH03 likely explain why the drifter trajectory is best captured with a value of 120° for θ. Though such a simplification does not yield perfect reconstructions of the Ekman velocity from wind stress measurements, we are confident that it is sufficient for the purpose of producing upper limits on the uncertainty of synthetic trajectories.

Synthetic trajectories are calculated within the surface velocity field by advecting a particle (that simulates either an observed surface drifter or a turtle) forward from its initial position using the simple product of the local instantaneous velocity and the length of the time step, which is one day. Geostrophic and Ekman velocities at a position between grid points are determined by bilinear interpolation in space using Shepard's (1968) method. Daily geostrophic velocity is obtained by linearly interpolating between the weekly geostrophic velocities. Temporal interpolation is not necessary for the Ekman velocity since the wind stress is already sampled at daily intervals. The synthetic trajectory is "launched" in the velocity field and then advected forward daily using the sum of geostrophic and Ekman velocities.

2.2. Incorporating uncertainty in the synthetic trajectory calculation

Since satellite-derived velocity fields are not currently able to resolve the characteristic length and time scales of mesoscale eddies,[3] the calculation of a synthetic trajectory must account for uncertainty due to the lack of information on subgrid-scale motions. This lack of information affects the calculation of the synthetic trajectories in two ways: there is uncertainty regarding the initial condition of the launch and there is uncertainty in the reconstructed velocity field that is integrated to produce the synthetic trajectory. Each of these sources is discussed in turn in this section.

Measurement uncertainty in the initial position of a turtle is dependent on the quality of the ARGOS fix and is typically anisotropic (Costa et al., 2010). Coupled with this uncertainty is the fact that we do not know the surface velocity fields at the exact time of the turtle's launch. In fact, our knowledge of this velocity is limited by the coarsest spatial scale of ½° (corresponding to the QuikSCAT spatial grid) and the coarsest temporal scale of one week (corresponding to the AVISO measurement interval). Thus, to incorporate uncertainty in the initial condition due to subgrid scale features in space and time, a grid box ½° in diameter centered at the initial position of the surface drifter or turtle is populated with nine evenly spaced launch points, from which trajectories are launched daily from three days before to three days after the initial time. The result is a seven-day repeat launch of nine trajectories from each initial position and is meant to represent the envelope of possible initial conditions within the underresolved velocity field. These choices are made here to demonstrate this method and can clearly be modified to weight the number of trajectory launches in space and time and/or modified to include calculated errors in the position fixes. For instance, Bailey et al. (2008) detail a method for finding the 95% error ellipse around the turtle position fixes using a state-space model that yielded mean uncertainties of 0.18° in latitude and 0.21° in longitude.

Uncertainty of the reconstructed velocity field along the drifter or turtle pathway is quantified by finding the standard deviations of both the Ekman and geostrophic velocities at each grid point and each time interval. Standard deviations for the geostrophic velocity field (sampled weekly) were computed with data over a two-month period centered on the time of interest. Standard deviations for the Ekman velocity field (sampled daily) were computed with data over a two-month period centered on the time of interest. Thus, each grid point in space and time has a velocity field with a measure of uncertainty.

The implicit assumption here is that the dominant error results from coarse grid scaling of reconstructed velocity data rather than measurement uncertainty in the data itself.

However, we do note that there is considerable altimetric measurement error in the estimates of the geostrophic current component. Section 3.2 also includes a discussion of the errors resulting from the choice of a simple model for reconstructing Ekman surface velocity. The uncertainty estimates utilized in this study are upper limits meant primarily to capture unresolved features in the velocity data in addition to measurement error. Future refinements to this method may include explicit measurement uncertainty into the along-track uncertainty measure.

As a synthetic trajectory is integrated forward in time, the reconstructed velocity field and its corresponding standard deviation field are interpolated to the location of the synthetic trajectory using the bilinear interpolation method mentioned in Section 2.1. At each step in the integration, a random velocity perturbation, produced using a Monte-Carlo approach, is added to the observed interpolated velocity. Random velocity perturbations are drawn from a standard normal distribution scaled by the local standard deviation of the velocity. Thus, the total velocity at each time step is given by

$$\vec{u} = \vec{u}_g + \vec{u}_e + \vec{\sigma}_g X + \vec{\sigma}_e Y \tag{2}$$

where u_g and u_e are the geostrophic and Ekman velocities, respectively, σ_g and σ_e are the standard deviations of the geostrophic and Ekman velocities, respectively, and X and Y are the random variables drawn from a standard normal distribution [$X \sim N(0,1)$; $Y \sim N(0,1)$].[4] Repeated launches produce different trajectories due to different "draws" from the velocity distributions. All synthetic trajectories are considered equally valid

[2] In the Pacific, within five degrees of the equator and along the South American coast, Ekman surface velocities may equal or exceed geostrophic velocities by a factor of two. In the rest of the Pacific Ocean, geostrophic velocities will typically exceed Ekman velocities by up to 50% or up to a factor of five in the vicinity of major surface currents.

[3] Stammer (1997) analyzed climatologies of Topex/Poseidon data and found eddies to have a spatial scale of 50–120 km and temporal scale of 1–6 days.

[4] Means of geostrophic and Ekman velocities almost always exceed their respective standard deviations. Near the equator the means exceed standard deviations by one–two orders of magnitude. The standard deviation of Ekman velocities (as calculated above) exceeds that of geostrophic velocities by up to an order of magnitude at the equator and near the Pacific coast of South America. Everywhere else, the standard deviation of geostrophic velocities is greater.

possibilities for the "true" trajectory. A test for the optimal number of trajectories necessary to accurately represent the spread of uncertainty in space and time revealed that the standard deviation of month-long synthetic trajectory locations stops increasing after the trajectory cloud is populated with ~1000 synthetic trajectories.

The use of initial launch envelopes and standard deviation as a measure of subgrid-scale uncertainty owes heavily to the well-established literature on Lagrangian Stochastic Modeling. Paris et al. (2005) utilized trajectory launch envelopes along with a number of biophysical metrics to model larval transport pathways from Cuban Snapper spawning aggregations. The methodology of Ullman et al. (2006) is similar to this study, whereby uncertainty is estimated using a Monte-Carlo approach with a velocity random walk. Following the theoretical work of Griffa (1996), Ullman et al. show that Eulerian standard deviation can be used as an estimate of subgrid-scale turbulent processes in real oceanographic applications.

2.3. Family of Linked Atlantic Model Experiments (FLAME)

Before applying the method described above to actual drifter and sea turtle tracks, a proof-of-concept is provided with application to high-resolution model data. Velocity output from the Family of Linked Atlantic Model Experiments (FLAME) (Biastoch et al., 2008) was used to simulate synthetic trajectories for our study. This model is run on a 1/12° spatial grid with half-hour integrations to produce a velocity field over the North Atlantic. The surface velocity output, provided at the native spatial resolution (1/12°) in three-day snapshots, is used to create synthetic trajectories from selected launch sites in the North Atlantic subtropical gyre. The drifters are advected using the native spatial resolution and hourly (linearly interpolated) time steps.

3. Results

3.1. Synthetic trajectories from FLAME output

To illustrate the impact of undersampled small-scale motions on the reconstruction of a pathway, trajectories are calculated using FLAME output at its native resolution (1/12°) as well as the FLAME output subsampled to 1/6°, 1/3° and 1° resolutions. In other words, FLAME model output is spatially subsampled to produce a series of trajectories. Fig. 2a demonstrates the information loss that occurs as a result of this subsampling. Predictably, eddies are poorly resolved at lower resolutions and the Lagrangian trajectory computed from subsampled fields significantly diverges from the "real" trajectory (black line) generated by velocity data at the native 1/12° resolution. At resolutions of 1/6° (red line) and 1/3° (blue line), small-scale features are sufficiently resolved such that the trajectories integrated with these lower resolution velocity fields are similar to the native resolution trajectory. Nonetheless, even at these resolutions, small differences with the native resolution will ultimately cause trajectories to diverge, as exhibited in Fig. 2a, where the 1/6° and 1/3° trajectories loop clockwise near their termination, a feature not exhibited by the "true" 1/12° trajectory.

Synthetic trajectories are produced from the model velocity fields subsampled at 1/3° since that resolution closely resembles the resolution of satellite-derived velocity fields. Following the method for incorporating uncertainty described in Section 2.2, a box 1/3° in diameter surrounding the initial launch location is populated with launch points that are released one day before and after the initial launch time of the deterministic trajectory. The three-day launch window is consistent with the temporal resolution of the FLAME model output. Standard deviations for the velocity field are produced at native resolution using a 45-day moving boxcar window. The resulting ensemble or "spaghetti plot" of synthetic trajectories (Fig. 2b) is superposed on the divergence of the model velocity field at day 112, when the trajectories diverge. In the area of strong divergence (near the center of the field, colored red) small differences in trajectory positions create sharply diverging pathways. Though such strong local features preclude a faithful reconstruction of the path of a surface drifter or turtle from a coarsely resolved velocity field, we note that over the first several weeks of the integrations, the reconstructed trajectories mimic the native resolution trajectory to a fair degree. However, without information about the "true" trajectory, the full spread of floats must be considered as the bounds of possible movement given the coarsely sampled fields.

3.2. Synthetic trajectories constructed from satellite data

Synthetic trajectories created for the passive drifter depicted in Fig. 1c are shown in Fig. 3c, while those created for the turtles

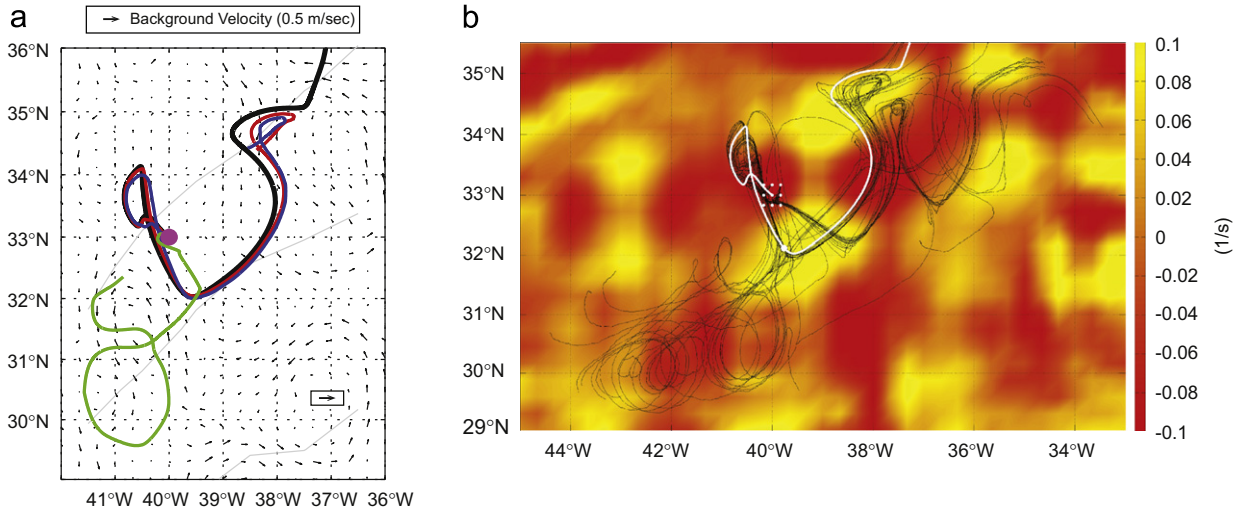

Fig. 2. (a) Deterministic trajectories for a launch (magenta dot) in the North Atlantic, integrated for 189 days by FLAME data subsampled to different resolutions: 1/12° (black), 1/6° (red), 1/3° (blue), and 1° (green). Background vectors denote the 1/3° velocity field at the time of launch. (b) Synthetic trajectories (magenta) integrated for 189 days using FLAME data shown with deterministic trajectory at native resolution (black). Trajectories are superposed on the divergence of the velocity field at day 112, indicated with a magenta dot. Fifty synthetic trajectories are shown, randomly selected from a total of 540.

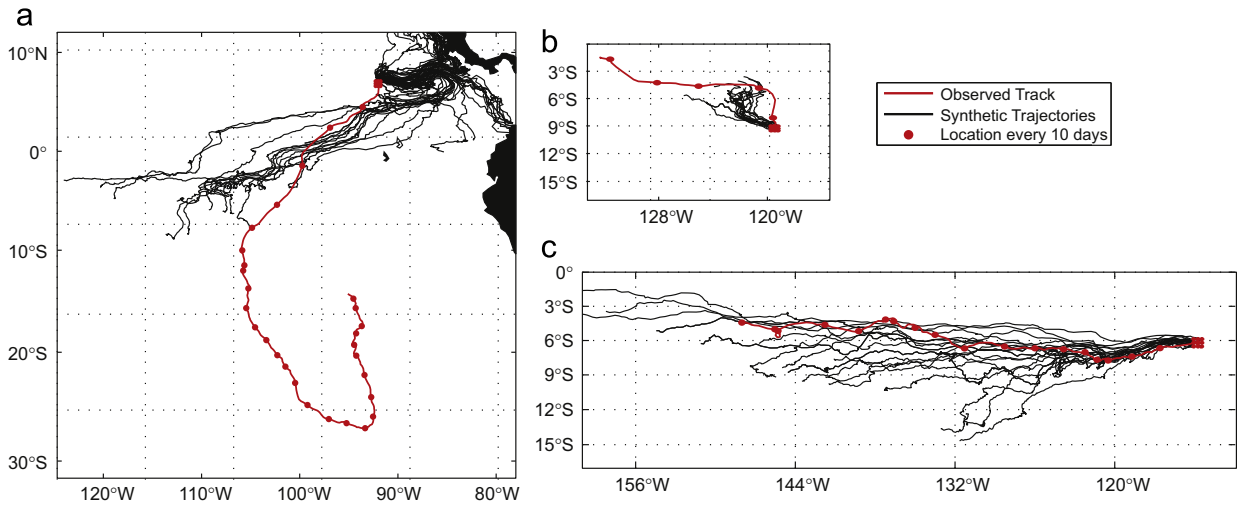

Fig. 3. Synthetic drifters (red) for the trajectories (black) shown in Fig. 1(a and b) observed sea turtles, (c) passive drifter. Fifty synthetic trajectories are shown, randomly selected from a total of 540. Black dots are placed every ten days along the observed tracks.

are shown in Fig. 3a and b. As shown in Fig. 3c, the observed passive drifter buoy stays within the trajectory cloud for several months, as expected. Additionally, 32 other passive drifter buoys were tested over a wide range of flow regimes throughout the subtropical Pacific and Atlantic. Over 90% of 896 observed drifter track-days fell within two standard deviations of the centroid of the synthetic trajectory cloud for one month after launch. In contrast, the observed turtle tracks in Fig. 3a and b exit their respective trajectory clouds in a matter of days. Once outside the trajectory cloud, these turtle trajectories cannot be plausibly explained by passive movement. Thus, we conclude that both turtle tracks exhibit active locomotion. Though this is a conclusion we might have made before with a minimal knowledge of the local surface velocity field, the cloud of synthetic trajectories provides a repeatable, rigorous method that can be applied for any section of the trajectory at any time, given corresponding satellite measurements of surface velocities.

One potential issue with the drifter and turtle trajectories chosen for this study is their location near the equator where geostrophy breaks down. This has been accounted for in the AVISO geostrophic velocity product. For a complete explanation, the reader is referred to http://www.aviso.oceanobs.com/es/services/faq/index.html. In the case of the trajectory in Fig. 3a, the sign of θ is reversed across the equator when reconstructing Ekman velocities with the method described in Section 2.1. This follows from Figure 8 of RH03, which shows how the sign of θ changes across the equator while the magnitude of θ remains constant.

We note, however, that if our method was a completely effective scheme for creating a spatial map of possible passive trajectories, the observed passive drifter track in Fig. 3c would remain at the centroid of the cloud indefinitely. Though the observed passive drifter remains inside the cloud for several months, there is some drift from the center of the synthetic trajectory cloud. Three explanations for the small systematic directional offset of synthetic trajectory clouds from observed drifter locations include a non-normal distribution of errors resulting from subgrid-scale uncertainty, bias introduced by the perturbations in initial position and time of trajectory launch and movement of the passive drifter drogue with subsurface velocities rather than the surface velocities reconstructed from satellite measurements. The latter explanation also sheds light on another potential source of uncertainty in observed turtle trajectories, namely, their weak dependence on subsurface velocities during turtle diving (Shillinger et al., 2011). Thus, the small divergence of the centroid of the synthetic trajectory cloud from the observed passive drifter over many months is likely due to the accumulation of errors over many time steps plus an imperfect fit for the parameters in the velocity reconstruction. As will be discussed in the next section, the accumulation of this error can be avoided by relaunching the synthetic trajectories at points along the observed trajectory.

3.3. Daisy chain method

The method discussed above for incorporating uncertainty into synthetic trajectories is based on a goal of projecting probable trajectories given an initial position and information on the surface velocity fields. However, this method does not utilize all available information since daily position fixes are available for the turtles and six-hour position fixes are available for the passive drifter. Utilizing this available information, the synthetic trajectory cloud is reinitialized to the observed location periodically, allowing a determination of whether a particular section of a trajectory is active or passive. Such a technique will produce a chain of trajectory clouds emanating from locations along the observed track. We term this technique as "daisy chain" method.

This method is utilized to produce a set of trajectory clouds (Fig. 4) for the three observed tracks in Figs. 1 and 3. Synthetic trajectories are relaunched on discrete time intervals from a launch box surrounding the observed position of the turtle. Thus from each position at regular intervals, a set of synthetic trajectories is produced. Rather than plotting all possible trajectories that emanate from each of these positions, contours encircling 50% (inner contour) and 95% (outer contour) of the final positions of the synthetic trajectories are plotted. These contours are color coded to match the observed position of the turtle or drifter at the end of the time interval. In other words, if a turtle's movement is passive, its observed position is expected to fall with the same colored contours marking the uncertainty limits. If the turtle's observed position falls outside these uncertainty limits, its motion can be assumed to be active.

In order to allow enough time between reinitializations of the trajectory cloud for a drifter or turtle to exit the populated box of initial trajectory positions, we have chosen to display daisy-chain figures with ten-day relaunches. Relaunch intervals are clearly a choice and should be guided by the speed of the drifter or turtle relative to the background noise of the velocity field and by the time scale of interest for different research questions. In the

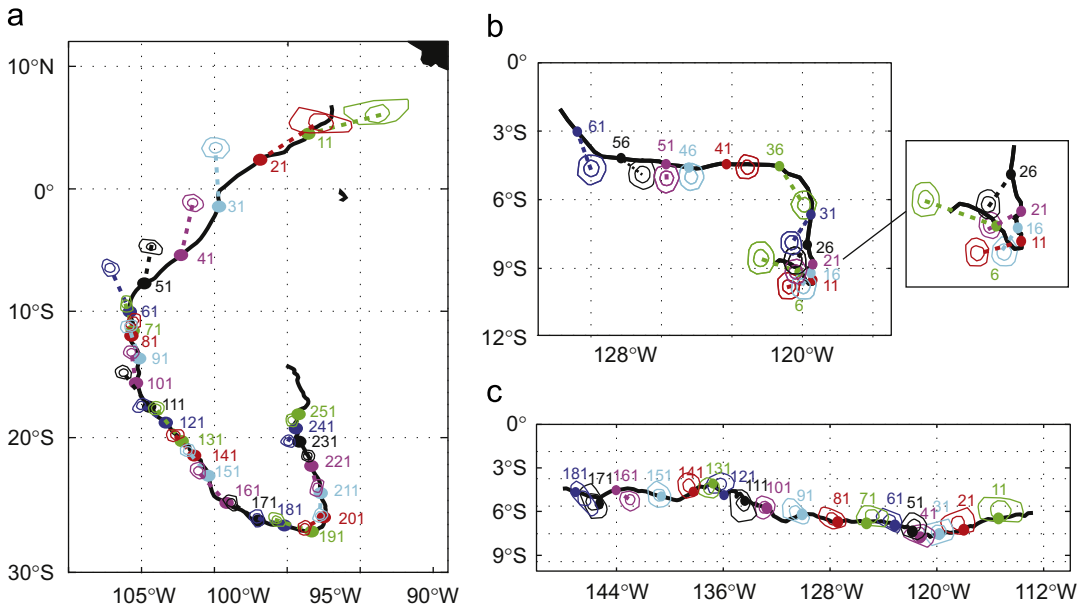

Fig. 4. Daisy chain method for the trajectories (black)shown in Fig. 1(a and b) observed sea turtles, (c) passive drifter. In (a) and (c) synthetic trajectory cloud was reinitialized every ten days. In (b) synthetic trajectory cloud was reinitialized every five days. The date of the observed locations are color coded to correspond to the contours enclosing 95% and 50% of predicted synthetic trajectories for that date.

interpretation of the plots in Fig. 4, each set of colored contours encloses the possible final positions of a passive drifter ten days from an observed location. The dot with the same color represents the observed location of the turtle (or actual drifter) 10 days from the prior set of colored contours.

The daisy chain technique may be tuned with two parameters: the time interval between relaunches and the length of time each ensemble of synthetic trajectories is simulated. Each parameter may be chosen to reflect the goals of a particular study. The highest-resolution limiting case is launching a daisy chain at every known turtle position and simulating trajectories until the 95% contour interval around the trajectory ensemble's endpoints is beyond the downstream turtle positions. This limiting case is very similar to the calculation of Finite Scale Lyaponov Exponents (FSLEs) along the turtle track, a recently developed Lagrangian analysis technique that has been proven to work well when comparing drifter tracks to velocity fields (Haza et al., 2007). Based on numerous trials with different launch intervals, we believe that our results are not especially sensitive to our choice of either the daisy chain reinitiation time or the length of time each daisy chain is simulated. Although an FSLE analysis of turtle tracks is beyond the scope of this paper, it is a natural extension of the daisy chain technique proposed here.

An examination of the passive drifter's trajectory (Fig. 4c) shows that with ten-day re-launches, the observed position of the passive trajectory almost always (with one exception on day 161) falls within the 95% contour of the synthetic trajectory cloud. This is the expected result, since the passive drifter's movement should be explained by the satellite velocity data and incorporated uncertainty. Additionally, we note that this result is expected given the calibration of θ to yield correspondence between the observed drifter trajectory and the cloud of synthetic trajectories, as discussed in Section 2.1.

The application of the daisy chain method to the turtle trajectory in Fig. 1a is illustrated in Fig. 4a. In this plot the 95% contour for the synthetic trajectories never aligns with the actual position of the turtle after ten days, indicating that the turtle's movement is not explained by the surface velocity field or its uncertainty during any ten-day interval of the track. Our conclusion is that this turtle exhibits active movement throughout the entire nine-month section of track trajectory displayed here.

Fig. 4a and c demonstrates that the daisy chain method provides results consistent with what would be expected given our previous knowledge of those two tracks. However, Fig. 4b, which shows the application of the daisy chain method to the trajectory in Fig. 1b, illustrates the advantage of this method over that illustrated in Fig. 3 where only information of the initial position was used. In Fig. 4b, there are sections of the track in which the synthetic trajectories correctly predict the position of the sea turtle (when the sea turtle position lies within the corresponding contour) and others when they do not. If the observed location falls within the 95% contour of synthetic trajectory positions (days 46–55), the null hypothesis is not rejected and the turtle's position can be explained by passive advection by surface currents. However, in the alternative scenario (days 1–45 and 56–66) the turtle exhibits movement not explained by the synthetic trajectories (to a 95% confidence) and is likely exhibiting active movement. Having some knowledge about the dynamics of this region, it is possible to conclude that the turtle is actively swimming most of the time, but when it enters the South Pacific Equatorial Current its movement is small compared to the passive transport being provided by the strong surface current.

4. Summary

The daisy chain maps developed in the last section offer a significant improvement over the full trajectory clouds (Fig. 3) for displaying the actual location of an observed trajectory relative to the envelope of possible locations for completely passive movement. As demonstrated above, these maps provide an operational method for evaluating segments of observed trajectories and determining the extent to which they display active or passive movement. The method described here is intended to be a starting point for any number of improvements. As mentioned above, there are known errors in the ARGOS satellite locations for

the turtles (Costa et al., 2010). A future development for our method would be to explicitly account for these position uncertainties using the uncertainties determined from the application of a state-space model (Jonsen et al., 2005; Bailey et al., 2008). However, continued development of more accurate tracking technology, such as Fastloc GPS tags (Rutz and Hays, 2009), will further improve our ability to determine animal locations and reduce the need for state-space estimates. Additionally, an important improvement would be to account for the uncertainty in the parameters of β and θ, as well as allow for the spatial and temporal variability of these parameters. The method developed here also involved choices that are clearly user-dependent or study-dependent. For example, the appropriate amount of time between relaunches of synthetic trajectories may depend entirely on the objectives of a specific study. The number of launches can also be varied, as can the temporal and spatial windows over which the launches are made.

The method proposed here is potentially useful for estimating high foraging success. However, it is just one of a suite of complimentary metrics of animal behavior that can be used in combination to identify foraging hotspots. In addition to those metrics mentioned in G06, Jonsen et al. (2007) and Fossette et al. (2010) have utilized data on diving behavior to independently verify patterns of foraging by leatherback turtles. Our method also has applications for assessing the extent of animal swimming, which may be important in determining the underlying navigational cues used in long-distance migration (Papi et al., 2000).

Finally, the method developed here for incorporating uncertainty in the velocity field used for the reconstruction of sea turtle pathways can be applied to a wide variety of other problems, such as pollution dispersal in the atmosphere or ocean and the optimization of search-and-rescue operations. Repurposing this method for such a variety of applications requires knowledge of the velocity field and a measure of its uncertainty in space and time.

References

Ardron, J., Gjerde, K., Pullen, S., Tilot, V., 2008. Marine spatial planning in the high seas. Mar. Policy 32, 832–839.

Bailey, H., Shillinger, G., Palacios, D., Bograd, S., Spotila, J., Paladino, F., Block, B., 2008. Identifying and comparing phases of movement by leatherback turtles using state-space models. J. Exp. Mar. Biol. Ecol. 356, 128–135.

Benhamou, S., 2004. How to reliably estimate the turtuosity of an animal's path: straightness, sinuosity or fractal dimension? J. Theor. Biol. 229, 209–220.

Biastoch, A., Böning, C.W., Getzlaff, J., Molines, J.M., Madec, G., 2008. Causes of interannual—decadal variability in the meridional overturning circulation of the mid-latitude North Atlantic Ocean. J. Clim. 21, 6599–6615.

Costa, D.P., Robinson, P.W., Arnould, J.P.Y., Harrison, A.L., Simmons, S.E., Hassrick, J.L., Hoskins, A.J., Kirkman, S.P., Oosthuizen, H., Villegas-Amtmann, S., Crocker, D.E., 2010. Accuracy of ARGOS locations of pinnipeds at-sea estimated using Fastloc. GPS. PLoS One 5, e8677.

Fossette, S., Hobson, V.J., Girard, C., Calmettes, B., Gaspar, P., Georges, J.Y., Hays, G.C., 2010. Spatio-temporal foraging patterns of a giant zooplanktivore, the leatherback turtle. J. Mar. Syst. 81, 225–234.

Game, E.T., Grantham, H.S., Hobday, A.J., Pressey, R.L., Lombard, A.T., Beckley, L.E., Gjerde, K., Bustamante, R., Possingham, H.P., Richardson, A.J., 2009. Pelagic protected areas: The missing dimension in ocean conservation. Trends Ecol. Evol. 24, 360–369.

Gaspar, P., Georges, J.Y., Fossette, S., Lenoble, A., Ferraroli, S., Maho, Y.L., 2006. Marine animal behaviour: Neglecting ocean currents can lead us up the wrong track. Proc. R. Soc. B 273, 2697–2702.

Godley, B.J., Blumenthal, J.M., Broderick, A.C., Coyne, M.S., Godfrey, M.H., Hawkes, L.A., Witt, M.J., 2008. Satellite tracking of sea turtles: Where have we been and where do we go next? Endang. Species Res. 4, 3–22.

Griffa, A., 1996. Applications of stochastic particles models to oceanography problems. In: Adler, R.J., Muller, P. (Eds.), Stochastic Modelling in Physical Oceanography. Birkhauser, Boston.

Haza, A.C., Griffa, A., Martin, P., Molcard, A., Ozgokmen, T.M., Poje, A.C., Barbanti, R., Book, J.W., Poulain, P.M., Rixen, M., Zanasca, P., 2007. Model-based directed drifter launches in the Adriatic Sea: Results from the DART Experiment. Geophys. Res. Lett., 34. doi:10.1029/2007GL029634.

Jonsen, I.D., Fleming, J.M., Myers, R.A., 2005. Robust state-space modeling of animal movement data. Ecology 86, 2874–2880.

Jonsen, I.D., Myers, R.A., James, M.C., 2007. Identifying leatherback turtle foraging behaviour from satellite telemetry using a switching state-space model. Mar. Ecol. Prog. Ser. 337, 255–264.

Papi, F., Luschi, P., Akesson, S., Capogrossi, S., Hays, G.C., 2000. Open-sea migration of magnetically disturbed sea turtles. J. Exp. Bio. 203, 3435–3443.

Paris, C.B., Cowen, R.K., Claro, R., Lindeman, K.C., 2005. Larval transport pathways from Cuban snapper (Lutjanidae) spawning aggregations based on biophysical modeling. Mar. Ecol. Prog. Ser. 296, 93–106.

Rio, M.H., Hernandez, F., 2003. High-frequency reponse of wind-driven currents measured by drifting buoys and altimetry over the world ocean. J. Geophys. Res. 108, 1–39.

Rutz, C., Hays, G.C., 2009. New frontiers in biologging science. Bio. Lett. 5, 289–292.

Shepard, D., 1968. A two-dimensional interpolation function for irregularly-spaced data. In: Proceedings of the 1968 23rd ACM National Conference/Annual Meeting, pp. 517–524.

Shillinger, G.L., Palacios, D.M., Bailey, H., Bograd, S.J., Swithenbank, A.M., Gaspar, P., Wallace, B.P., Spotila, J.R., Paladino, F.V., Piedra, R., Eckert, S.A., Block, B.A., 2008. Persistent leatherback turtle migrations present opportunities for conservation. PLoS Biol. 6, e171.

Shillinger, G.L., Swithenbank, A.M., Bograd, S.J., Bailey, H., Castelton, M.R., Wallace, B.P., Spotila, J.R., Paladino, F.V., Piedra, R., Block, B.A., 2010. Identification of high-use internesting habitats for eastern pacific leatherback turtles: Role of the environment and implications for conservation. Endang. Species Res. 10, 215–232.

Shillinger, G.L., Swithenbank, A.M., Bailey, H., Bograd, S.J., Castelton, M.R., Wallace, B.P., Spotila, J.R., Paladino, F.V., Piedra, R., Block, B.A., 2011. Vertical and horizontal habitat preferences of post-nesting leatherback turtles in the South Pacific Ocean. Mar. Ecol. Prog. Ser. 422, 275–289.

Stammer, D., 1997. Global characteristics of ocean variability estimated from regional TOPEX/POSEIDEN altimeter measurements. J. Phys. Ocean 27, 1743–1769.

Ullman, D.S., O'Donnell, J., Kohut, J., Fake, T., Allen, A., 2006. Trajectory prediction using HF radar surface currents: Monte Carlo simulations of prediction uncertainties. J. Geophys. Res. 111, C12005.